

INVESTIGATION OF MECHANICAL PROPERTIES OF Al 6063 ALLOY NANO-COMPOSITES

K. R. SATYANARAYANA
Research scholar, Dept. of ME,
GITAM University, India
satya_1171@rediffmail.com

Dr. B. SURENDRA BABU
Professor,
Mechanical Engineering, GITAM
University, India

Dr. B. RAMESH CHANDRA
Assistant Professor,
Mechanical Engineering, JNTUH
COE, India

Dr. M. NAGENDRABABU
Assoc. Prof., Dept. of Mechanical
Engineering, VIEW, India. (HSSOE,
University of California Los Angeles, LA,
CA, USA -90017)

Dr. G. SWAMI NAIDU
Professor,
Dept. of Metallurgical Engineering,
JNTUV, India

ABSTRACT

Microstructural characterization of Al6063 Nano composites plays a vital role in the field of Materials Engineering. Many of the earlier researches showed that the evolution of Al6063 stabilized the application in wide fields of engineering and sciences. Present research has focused to probe the Al6063 nano composite using Electrical Resistivity, Strength tests, Wear characterization, Coefficient of Thermal Expansion, Machinability studies and Damping behavior. Compositions of Al6063, Al6063 with 0.5 wt% γ -Al₂O₃, 1 wt% γ -Al₂O₃, 2 wt% γ -Al₂O₃ and 3 wt% γ -Al₂O₃ were prepared and investigated for various mechanical properties. In aggregate to investigation of mechanical properties the nano powder particles forms apparently bonds and they show higher strengths. Instead of chemical reactions, nano particles implicated the improvements in higher fracture toughness in Al 6063 + 2 wt% γ -Al₂O₃ than other compositions. In Fracture test of Al 6063 + 3 wt% γ -Al₂O₃, the nano particles were widely spread and showing higher fracture toughness.

Keywords: Electrical resistivity, Material Science, Nano Materials, Damping, Thermal Expansion, Fracture Toughness.

INTRODUCTION

Controlled by one direction solidification base alloys may result in multi-phase or heterogeneously distributed microstructure in the matrix. In this process of dispersion fillers is matrix alloys and rainfall during freezing point. Crucible is filled with alloys moves downwards, melting and pour point is under the standard conditions.

(Majzoobi, Nemati, Pipelzadeh, & Sulaiman, 2016) It follows from this that this process improves the properties Eutectic alloy super system. The main advantages are enhanced bar strength at high temperatures, low flow and thermal stability microstructure. (Faregh & Hassani, 2017). Manufacture both matrix aluminum alloy and strengthening, powders and even the mixing ball mill has been used. And Production MMCs was realized by sintering and mixing wet process. This method provides the necessary uniform solid distributed microstructure and mechanical properties and there will be no secondary activities. (Wang, Zhao, & Zhang, 2017) Limit powder metallurgy technology is a bad wettability between the housing and metal powders because of absence of interaction in liquid form. Another major problem in this method, the dispersion Nano-ceramic phase uniformly in the matrix aluminum alloy. (Majzoobi, Nemati, Pipelzadeh, & Sulaiman, 2016)

MATERIALS & METHOD

Specimen Fabrication

Samples have been prepared on the implementation cuts, grinding and polishing, which can then after etching for examination in accordance with ASTM F2450-04.

Table 1. Al6063 Composition

S.No	Metal	Wt% Composition
1	Al	Base
2	Cu	3.5
3	Mg	1.02
4	Fe	0.93
5	Mn	0.59
6	Si	0.44
7	Zn	0.38
8	Pb	0.1
9	Ti	0.04
10	Cr	0.03
11	Co	0.005
12	Ni	0.005
13	Bi	0.004

Steps necessary to the production of Nano Al₂O₃ reinforced metal matrix composites using stir casting (liquid metallurgy techniques).

- Exercise for the casting.
- Degassing of molten metal by rinsing clean argon gas in order to create an inert atmosphere to prevent oxidation.
- Supplying calculated amount of super-heated liquid molten metal to mixing chamber.
- Supplied calculated amount of preheated Nano Al₂O₃ particles in the mixing chamber.
- An immediate shake and pour into a form.
- Finished model has been removed from the distribution will die.
- Extra and unwanted material model has been removed from the cleaning process.

MECHANICAL PROPERTIES

Electrical Conductivity / Resistivity

Electrical conductivity/resistivity is to a large extent examined properties in the field of research materials. There are several applications, such as high electrical/ thermal conductivity metals and alloys, exploited. Study electrical behavior metal matrix composites, it is important when these characteristics must be combined with good mechanical properties. Metal matrix composites have high electrical conductivity due to the

presence of electrons as charge carriers. In the analysis MMNC resistivity, specific resistance is generally considered to be an order of magnitude of more than matrix alloys from the chassis is usually ceramic material. It follows that the electrical resistance, there is no point in the implementation process. Further, growth, rainfall and structural shortcomings largely influence electrical properties MMNCs.

Damping studies

Damping properties have been studied using two methods:

a. PUCOT Method

Preliminary dynamic modulus values were calculated on the basis of the forecast value Poisson's ratio 0.3 and the values dynamic Young's modulus (E) they have been obtained. Specimens are decorated with low saw speed. Dynamic Measurement module flexibility, control and amplitude at each of the samples shall be carried out with piezo ultrasonically composite oscillator (PUCOT).

b. Resonance Bar method

High damping capacity and light metals have potential use in weight critical structures, such as airlines, automotive applications. Quantity (E/d) 1/2, E - module flexibility and ρ - Density, means for higher specific rigidity, leads to a higher frequency and high damping capacity.

Particles reinforced MMNCs are one of the most important ways of low weight high rigidity structure.

Coefficient Thermal expansion

Coefficient thermal expansion of composite materials as well as concrete matrix alloy is determined using a Heat Mechanical Analyzer (TMA) display.

TMA instrument consists of the oven for heating sample and can work in the range from -70°C to 1200 °C. Sample is mounted on the bottom of a sample holder which are inserted into the oven. Thermocouple and crossing is located in close contact with the sample temperature recording. Temperature resistant quartz probe shall be carried out on a sample at one end and the other end is attached to a linear variable

differential transformer (location LVDT positioning for). This probe registers and transfer any small changes in motion. Moving Kernel location LVDT positioning for senses positive and negative tolerances probe to the template. As a model expands, or a contract or otherwise force exerted by the mass to be fundamental probe moves in annular space to accommodate LVDT positioning for. This relative movement creates a voltage change that is proportional to linear displacement core. Signal is amplified and processed on the computer data recording system. At the two ends samples have been polished with different grain of silicon carbide papers followed by fine polishing with 1mm diamond paste. The six NMCs samples have been tested. These data were obtained in the form dimensional changes as a function of temperature in the range of 30°C-300°C, and so in the fields of heating and cooling. Thermal expansion of (CTE) values have been established on calculated slope between the two selected temperatures of dimension change compared to heat waves.

Fracture toughness

A maximum load of 2KN and minimum load of 0.6KN was maintained throughout the test during fatigue loading. The process of introducing a crack with a plastic zone at the vicinity of the notch with the influence of fatigue load is called fatigue pre-cracking. In pre-cracking, a crack of length $a_p = 2.99\text{mm}$ is introduced. For the ratio $a/W = 0.511$, $f(a/W)$ is noted down as 9.96 for further validations.

Wear test

Wear samples shall be tested in the dry state. Common methods used to estimate wear sample losses are dimension method, the method shift, and loss of weight and wet clothes. Sample shall be weighed and the weight is registered. Guiding the sliding distance constant; sliding pressure to increase the load capacity and conducting the test. Target weight. The apparatus consists of rotary disc (EN24 steel with a hardness BHN 229) with diameter of 200 mm, which is opposite,

test samples or insert pins. Adjustments were made on samples and for the application of designs.

Machinability Test

Standard Cutting tests have been carried out by turning samples for CNC lathe. Cutting speed selected, 200, 315, 400 and 500 rpm. Cutting depth is 0,2, 0,5, 0,8 and 1 mm, feed-courses 0.1, 0.2, 0.32 and 0.4 mm/rev. Meanwhile, cutting forces (namely touches, axial and radial forces) were measured lathe tool dynamometer.

RESULTS AND DISCUSSIONS

Electrical Resistivity

Table 1: Electrical Resistivity ($\mu\Omega\text{cm}$) of Al and Al/Nano MMNCs)

Time (hrs)	% of Nano Composition				
	0	0.5	1	2	3
0.01	4.370	4.389	4.491	4.586	4.682
0.05	4.817	5.148	5.600	5.746	5.884
0.1	5.264	5.908	6.709	6.905	7.023
0.2	5.711	6.458	6.612	6.841	6.979
0.4	6.157	6.358	6.529	6.700	6.867
0.6	6.152	6.196	6.437	6.611	6.797
0.8	5.929	6.075	6.346	6.509	6.687
1	5.852	5.944	6.257	6.406	6.616
2	5.739	5.813	6.167	6.304	6.416
4	5.624	5.682	6.077	6.202	6.320

Changing electrical resistance with lid to 180°C for Al 6063 matrix alloys and Al/nano particles reinforced MMNCs. In the initial phase is a rapid increase in resistivity, at the next stage during which resistivity almost constant with aging and, in the final stage of slowly declines with age. A slight difference in duration of first phase resistance changes between materials, except that the Volume resistivity of composite materials is more than matrix. However, the middle level of composite materials is significantly less than on the basis alloy. Resistance in the composite materials for a longer period of aging in the final stage falling faster than concrete alloy.

Strength test

Results of the surroundings tensile tests are listed in table 5.2 and its engineering-strain waves are shown in Fig. 5.4(a) to (f). Land with 0.2% yield stress (σ_y), Strength (σ_u), the percentage elongation (%) and Young's modulus (E) as a function wt % reinforcement in the matrix. It was found that the values (0.2% YS (Document of stress, UTS AND YY) developed MMNCs increases in strengthening appendices 9 wt % with a modest reduction elongation (elongation nuts alloy is 5.36% and MMNCs is 4.04% (for 9 wt % Nano) and then by adding reinforcement above this limit the force deteriorates values. Increase 0.2% YS, UTS and modulus developed MMNCs containing 9 wt. % Nano particles are 2842 includes %, 22 % and 52 %, when compared to un-reinforced with ground. To increase strength in tension nanocomposites can be attributed to increase in the threshold grain in the grain refinement.

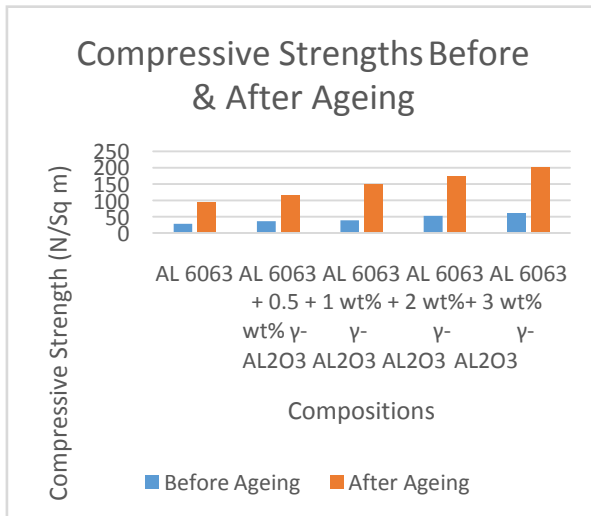


Figure 1 Chart illustration of Compressive strengths of various compositions

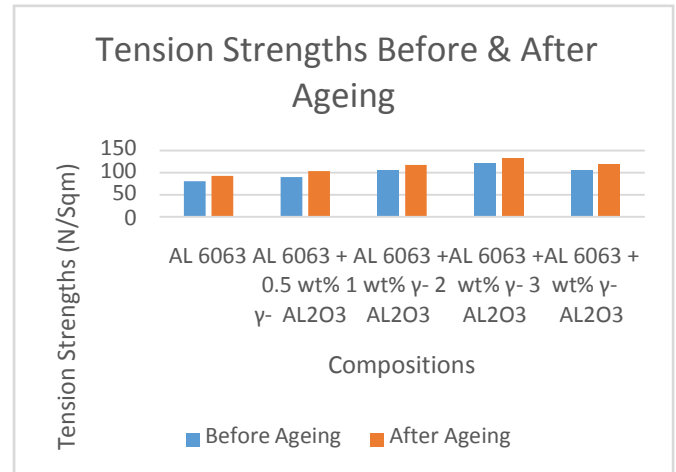


Figure 2. Chart Illustration of Tension Strengths of various compositions

Fracture toughness

Results of the investigations carried out on the basis of the refractive index interms K_{Ic} developed NMMCs and alloys. Land K_{Ic} & K_{max} as a function wt. % nano are shown in Figure. It is observed from these results, which are growing in strengthening the content in the matrix aluminum alloy have shown increased to a MMNCs up to 3 wt. % beyond this limit further addition reinforcement in the matrix aluminum alloy, a trend toward a nanocomposites. Despite the fact that it cannot be concluded that reinforced materials are weaker than concrete reinforcing materials, as can be seen from the results.

Table 2: Fracture Toughness Results

SNo	Composition	Pq	Pmax	a	F(a/W)	Kq	Kmax
1	Al 6063	1.872	2.054	12.7	9.66	8.957	9.826
2	Al 6063 + 0.5 wt% γ - Al ₂ O ₃	1.912	2.092	12.7	9.66	9.146	10.007
3	Al 6063 + 1 wt% γ - Al ₂ O ₃	1.98	2.097	12.7	9.66	9.473	10.031
4	Al 6063 + 2 wt% γ - Al ₂ O ₃	2.242	2.36	12.7	9.66	10.725	11.287
5	Al 6063 + 3 wt% γ - Al ₂ O ₃	2.005	2.15	12.7	9.66	9.592	10.28

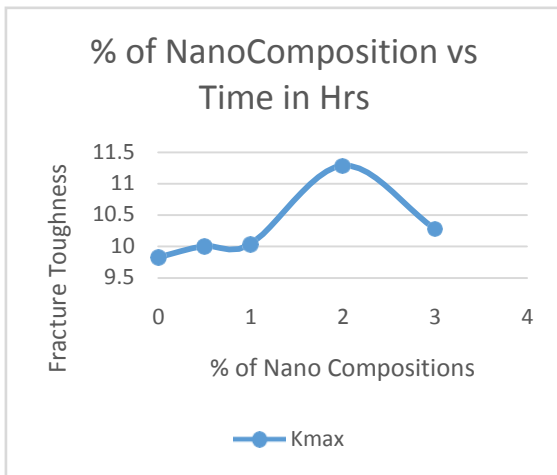


Figure 3. Chart Illustration of Fracture Toughness Results

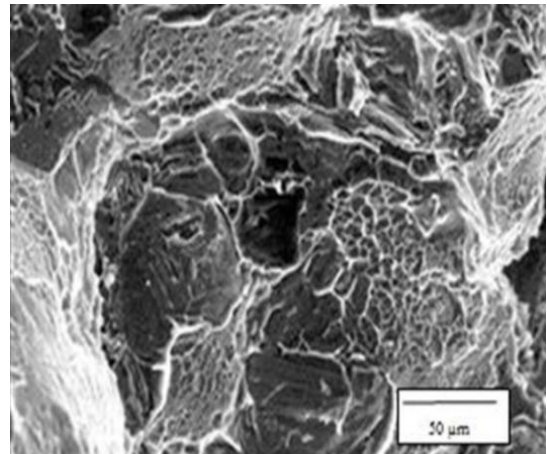


Figure 4. Fractograph SEM of Al 6063 + 3 wt% γ -Al₂O₃

Wear characterization

In this loss of material after test is calculated.

Table 3: Wear Mechanism Test Results

Chemical Composition	Before Ageing			After Ageing		
	Initial Weight (Grams)	Final Weight (Grams)	Wear Loss (Grams)	Initial Weight (Grams)	Final Weight (Grams)	Wear Loss (Grams)
AL 6063	98.23	97.86	0.79	97.14	96.67	0.47
AL 6063 + 0.5 wt% γ - Al ₂ O ₃	98.68	98.47	0.21	99.21	99.14	0.07
AL 6063 + 1 wt% γ - Al ₂ O ₃	98.67	98.6	0.26	97.22	96.91	0.31
AL 6063 + 2 wt% γ - Al ₂ O ₃	98.62	98.27	0.35	97.37	97.2	0.17
AL 6063 + 3 wt% γ - Al ₂ O ₃	97.12	96.43	0.69	96.98	96.33	0.65

Expressed Archard right to carry the equation, which says that wear rate increases linear with an increase in pressure and load. In fact, with the load, hard asperities on the disc penetrates the softer surface contact that distortions and fracture asperities for a smoother contact surface increases. Thanks to the increased accumulation, softer material from the surface gets into the valley between asperities area counter in turn reduces asperities height with the counter -surface and thus reduces performance during the cutting area counter asperities. Further increase the burden on begins subsurface and micro cracks. Combination of all these factors listed above shall contribute to the effective wear surface of the test piece.

Damping

To the flexibility and Poisson's ratio of PUCOT data listed in the table and in Figure below and the data in the 11% rule of mixtures. Bottom percentage difference % occurred in and a high percentage porosity in this specimen. This indicates that control interface can be a considerable part of decay in this specimen. It should be noted that elastic equation $E=2G(1 - \mu) E$, G, and cumulative Poisson's ratio assumes that material is flexible active. But developed materials are active. Despite the fact that the calculated values Poisson's ratio in the range 0.3 to 0.734, which is sufficient scope for Al 6063 nano-materials. Dependency module flexibility in the percentage nano in each sample is shown in the table below. Rule mixture

line connecting the two extremes and wave data points to composites. This trend is confirmed by the fact that nano is modulus

decreases linear and shall follow rule of mixtures.

Table 4. Strain Amplitude Evaluations

SNo	Composition	Strain Amplitude							
		10 ⁻⁷	10 ⁻⁶	10 ⁻⁵	10 ⁻⁴	10 ⁻³	10 ⁻²	10 ⁻¹	10 ⁰
1	AL 6063	2.732	2.921	3.066	3.200	3.256	3.323	3.367	3.457
2	AL 6063 + 0.5 wt% γ - AL ₂ O ₃	2.955	2.977	3.178	3.267	3.323	3.356	3.579	3.680
3	AL 6063 + 1 wt% γ - AL ₂ O ₃	2.977	3.033	3.222	3.323	3.356	3.479	3.680	3.802
4	AL 6063 + 2 wt% γ - AL ₂ O ₃	3.133	3.089	3.312	3.378	3.412	3.535	3.847	3.992
5	AL 6063 + 3 wt% γ - AL ₂ O ₃	3.256	3.144	3.390	3.434	3.457	3.613	4.003	4.159

PUCOT has been an effective way to determine the flexibility and strength, patterns. Thermal cycles of composite materials under T_g should not distinguish impact of density, dynamic young's module and modulus in bending, increasing by 56%. Thermal cycles of composite materials over T_g reduce density around 0.5 %, prices young"with module by 8 %, elastic modulus in bending by 15% and increase rigidity by 60%. This large increase damping is attributed to an increase of body cavities and cracks due to interface. Decay measurement are much more sensitive than measurement of density or elastic modules to monitor microstructural damage in Nano/Al matrix composites. Thermal processing cycle 784 cycles at 700°C is causing significant deterioration in fiber. In general, these studies have shown that the potential of this composition material is limited at 400 °C and for short-term exposure at this temperature.

Coefficient of Thermal Expansion

Variations in PLC MMCs with different weight percent nano amplification temperature is shown in figure below. It is clear that all waves SPS versus temperature for MMNCs with different percentage by mass of reinforcement should be similar characteristics, all waves show similar trends. During the heating of cycle as the temperature rises, and thus the PLC to return (cooling) part of the cycle, there is always some hysteresis and SPS at each temperature is always less than in the

heater. The hysteresis is more serious than nano content increases. Thermal Expansion Al6063 nut alloys and composites to the Nano as investigated in the temperature range of 25 °C to 500 °C, in the fields of heating and cooling.

CONCLUSION

Change microhardness and electrical resistance of composite materials as a function of time aging at a certain temperature aging supports the following sequence for the aging of such materials, which is similar to that which has been obtained from other researchers. At the start of the aging, supersaturated solid solution is transformed into a needle-shaped zone β -View" (cube directions matrix $\langle 100 \rangle$) β' continuous precipitate (rod-shaped precipitate is situated along $\langle 100 \rangle$) β -View (Mg₂a) balance precipitates (in the form incoherent platelets or discs), which was previously thought by several investigators from Al alloy 6063 system GP zone₂₄. In β'' and β''' phase particles are more resistance to movement or dislocations. It was also found that MMNCs containing 3 wt% registered the highest fracture toughness of 19.7% higher compared with concrete matrix aluminum alloy. Increase the refractive index developed MMNCs should be primarily attributable to presence and even distribution hard Nano particles in the Al matrix. Bringing together and the repression reinforcement with ground. These results indicate that the ageing and precipitation kinetics in the

matrix alloy is significantly accelerated due to the presence of reinforcement.

REFERENCES

- [1] Abdulstaar, M., Al-Fadhlah, K., Characterization, L.-M., & 2017, u. (n.d.). *Microstructural variation through weld thickness and mechanical properties of peened friction stir welded 6061 aluminum alloy joints*. Elsevier.
- [2] Agrawal, A., R.-T., & 2017, u. (n.d.). *End forming behaviour of friction stir processed Al 6063-T6 tubes at different tool rotational speeds*. journals.sagepub.com.
- [3] Agrawal, A., Narayanan, R., & Kailas, S. (2017, 10 4). *End forming behaviour of friction stir processed Al 6063-T6 tubes at different tool rotational speeds*. *The Journal of Strain Analysis for Engineering Design*, 52(7), 434-449.
- [4] Faregh, S., & Hassani, A. (2017, 3 1). *Stress and strain distribution in twist extrusion of AA6063 aluminum alloy*. *International Journal of Material Forming*.
- [5] Faregh, S., Forming, A.-I., & 2017, u. (n.d.). *Stress and strain distribution in twist extrusion of AA6063 aluminum alloy*. Springer.
- [6] Guo, B., Zhang, Z., International, R.-N., & 2018, u. (n.d.). *Ultrasonic and eddy current non-destructive evaluation for property assessment of 6063 aluminum alloy*. Elsevier.
- [7] Karthikeyan, A., Engineering, S.-I., & 2017, u. (n.d.). *Experimental analysis on sliding wear behaviour of aluminium-6063 with SiC particulate composites*. *Trans Tech Publ*.
- [8] Keshavamurthy, R., Sudhan, J., Gowda, N., & Krishna, R. (2016, 9). *Effect of Thermo-Mechanical Processing and Heat Treatment on the Tribological Characteristics of Al Based MMC's*. *IOP Conference Series: Materials Science and Engineering*, 149, 012118.
- [9] Ma, Z., Feng, A., Chen, D., & Shen, J. (2017, 9 18). *Recent Advances in Friction Stir Welding/Processing of Aluminum Alloys: Microstructural Evolution and Mechanical Properties*. *Critical Reviews in Solid State and Materials Sciences*, 1-65.
- [10] Ma, Z., Feng, A., Chen, D., State, J.-C., & 2017, u. (n.d.). *Recent Advances in Friction Stir Welding/Processing of Aluminum Alloys: Microstructural Evolution and Mechanical Properties*. Taylor & Francis.
- [11] Majzoobi, G.-H., Nemati, J., Pipelzadeh, M., & Sulaiman, S. (2016, 4 2). *Characterization of mechanical properties of Al-6063 deformed by ECAE*. *The International Journal of Advanced Manufacturing Technology*, 84(1-4), 663-672.
- [12] Singh, C., Singh, J., & Singh, R. (2018). *The effect of post welded heat treatment on mechanical properties and microstructure of friction stir welded Al 6063*.
- [13] Singh, R. (2018). *Characterization of microstructure and mechanical properties of AL6063 using FSP Multipass*. Anchor Academic Publishing.
- [14] Wang, C., Gao, Y., Wang, R., Wei, D., Cai, M., and, Y.-J., & 2018, u. (n.d.). *Microstructure of laser-clad Ni60 cladding layers added with different amounts of rare-earth oxides on 6063 Al alloys*. Elsevier.
- [15] Wang, Y., Zhao, S., & Zhang, C. (2017, 9 14). *Microstructural Evolution of Semisolid 6063 Aluminum Alloy Prepared by Recrystallization and Partial Melting Process*. *Journal of Materials Engineering and Performance*, 26(9), 4354-4363.
- [16] Wang, Y., Zhao, S., and, C.-J., & 2017, u. (n.d.). *Microstructural Evolution of Semisolid 6063 Aluminum Alloy Prepared by Recrystallization and Partial Melting Process*. Springer.